LBL-33760
UC-413

Lawrence Berkeley Laboratory
UNIVERSITY OF CALIFORNIA

Presented at the Ninth International Conference on Hyperfine Interactions, Osaka, Japan, August 17–21, 1992, and to be published in the Proceedings

Production of Unstable Nuclei Far from Stability Line—Its Scope and Limitations

K. Matsuta, A. Ozawa, Y. Nojiri, T. Minamisono, M. Fukuda, S. Momota, T. Ohtsubo, S. Fukuda, K. Sugimoto, I. Tanihata, K. Yoshida, K. Omata, J.R. Alonso, G.F. Krebs, and T.J.M. Symons

August 1992

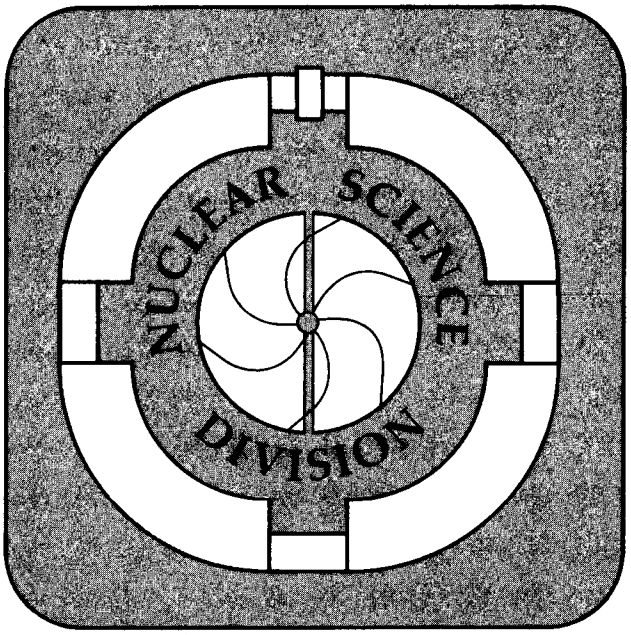

REFERENCE COPY
Does Not
Circulate
LBL-33760
Copy 1
Bldg. 50 Library.

Prepared for the U.S. Department of Energy under Contract Number DE-AC03-76SF00098

DISCLAIMER

This document was prepared as an account of work sponsored by the United States Government. Neither the United States Government nor any agency thereof, nor The Regents of the University of California, nor any of their employees, makes any warranty, express or implied, or assumes any legal liability or responsibility for the accuracy, completeness, or usefulness of any information, apparatus, product, or process disclosed, or represents that its use would not infringe privately owned rights. Reference herein to any specific commercial product, process, or service by its trade name, trademark, manufacturer, or otherwise, does not necessarily constitute or imply its endorsement, recommendation, or favoring by the United States Government or any agency thereof, or The Regents of the University of California. The views and opinions of authors expressed herein do not necessarily state or reflect those of the United States Government or any agency thereof or The Regents of the University of California and shall not be used for advertising or product endorsement purposes.

Lawrence Berkeley Laboratory is an equal opportunity employer.

DISCLAIMER

This document was prepared as an account of work sponsored by the United States Government. While this document is believed to contain correct information, neither the United States Government nor any agency thereof, nor the Regents of the University of California, nor any of their employees, makes any warranty, express or implied, or assumes any legal responsibility for the accuracy, completeness, or usefulness of any information, apparatus, product, or process disclosed, or represents that its use would not infringe privately owned rights. Reference herein to any specific commercial product, process, or service by its trade name, trademark, manufacturer, or otherwise, does not necessarily constitute or imply its endorsement, recommendation, or favoring by the United States Government or any agency thereof, or the Regents of the University of California. The views and opinions of authors expressed herein do not necessarily state or reflect those of the United States Government or any agency thereof or the Regents of the University of California.

LBL - 33760

PRODUCTION OF UNSTABLE NUCLEI FAR FROM STABILITY LINE — ITS SCOPE AND LIMITATIONS —

K. Matsuta, A. Ozawa, Y. Nojiri, T Minamisono, M. Fukuda, S Momota, T. Ohtsubo, S. Fukuda, K. Sugimoto, I Tanihata,[A] K. Yoshida,[A] K. Omata,[B] J.R. Alonso,[C] G.F.Krebs,[C] and T.J.M. Symons[C]

Department of Physics, Osaka Univ., Toyonaka, Osaka 560, Japan

(A) RIKEN, Wako, Saitama 351-01, Japan

(B) INS, The Univ. of Tokyo, Tanashi, Tokyo 188, Japan

(C) Lawrence Berkeley Laboratory, Berkeley, CA 94720, USA

August, 1992

This work was supported in part by the Director, Office of Energy Research, Division of Nuclear Physics of the Office of High Energy and Nuclear Physics of the U.S. Department of Energy under Contract DE-AC03-76SF00098

Printed on recycled paper

PRODUCTION OF UNSTABLE NUCLEI FAR FROM STABILITY LINE -ITS SCOPE AND LIMITATIONS-

K. Matsuta, A. Ozawa, Y. Nojiri, T. Minamisono, M. Fukuda, S. Momota, T. Ohtsubo, S. Fukuda, K. Sugimoto, I. Tanihata,[A] K. Yoshida,[A] K. Omata,[B] J.R. Alonso,[C] G.F. Krebs,[C] and T.J.M. Symons[C]

Department of Physics, Osaka Univ., Toyonaka, Osaka 560, Japan

(A) RIKEN, Wako, Saitama 351-01, Japan

(B) INS, The Univ. of Tokyo, Tanashi, Tokyo 188, Japan

(C) Lawrence Berkeley Laboratory, Berkeley, CA 94720, USA

Abstract Recent improvements in isotope separators can be utilized along with the availability of a wide range of nuclear species from the heavy-ion fragmentation process to study hyperfine interactions. We have measured the magnetic moments of mirror nuclei using this method at the Lawrence Berkeley Laboratory's Bevalac heavy-ion accelerator. We present the merits, applicability and limitations of the technique.

1. INTRODUCTION

For the study of hyperfine interactions detecting nuclear radiation, radioactive nuclear probes are crucial. Such isotopes have been produced through low energy nuclear reactions for long time. Since the construction of ISOLDE [1] at CERN, this type of facilities have been used for a wide range of studies. This method has been found attractive because of the relatively fast analysis capability, by combining the

on-line mass separator with the universal production method using high energy proton spallation. Although such ISOL [1] (Isotope Separator On-Line) facilities have a long history of providing a variety of isotopes, the method has limitations on available isotopes in terms of their chemical properties and lifetimes and on available kinetic energies of the nuclei necessary for deep implantation. The lower kinetic energy becomes a crucial problem, in some cases such as in Tilted Foil polarization experiments. Post acceleration of the separated isotopes makes the technique more powerful solving this kinetic energy problem, but other problems remain. Recoil separator combined with the production through low energy nuclear reactions gave another technique to have even faster analysis capability. Such a recoil separator has been applied to the measurement of magnetic moment of ^{33}Cl at Rochester [2].

For relatively light nuclei, the projectile fragmentation process in high energy heavy ion collisions provides another promising technique for the production of probe nuclei in a wide range of the nuclear chart. Combined with a fragment separator, application of this production technique is easy because of the high kinetic energy. The technique has been applied to the study of nuclear structure, and has led to various discoveries, including new isotopes [3], decay properties [4], and neutron halo in ^{11}Li covering ^{9}Li core [5].

The production and separation technique is powerful also for the study of hyperfine interactions on short lived nuclei because of its fast analysis capability. We have been using the projectile fragment nuclei as probes for β-NMR studies at the Lawrence Berkeley Laboratory's (LBL) Bevalac heavy ion accelerator. Polarization necessary for the studies can be created in such fragments either by the tilted foil technique (TFT) or through polarization phenomena in heavy ion collisions. Nuclear magnetic moments have been studied using such a combined

technique. In addition, a modified NQR technique [6,7], which was recently developed from the conventional β-NMR technique, will make even the quadrupole moment measurement possible. The present technique is useful also for any other β-NMR studies on the hyperfine interactions of radioactive impurities in various materials including ferromagnetic samples. It will be soon applied not only to these important hyperfine studies, but also to the study of basic symmetries in weak nucleon currents, such as determination of the Fermi coupling constant C_V in nuclear beta decay for spin non-zero nuclei.

In the following sections, the basic character, scope and limitations of the present technique are discussed.

2. PRODUCTION TECHNIQUE

The projectile fragmentation process in high-energy heavy-ion collisions combined with a fragment separator is powerful tool allowing the study of a wide range of nuclei. The basic technique was first introduced and was established at the LBL's Bevalac. After this superior technique was proven to be useful, many of similar facilities were built all over the world. Advantages of this method are, of course; 1. the projectile fragmentation process in the high-energy heavy-ion collisions produces a variety of nuclei in large quantities, 2. it has no elemental selectivity, 3. very fast analysis, on the order of micro seconds, 4. high kinetic energy.

a) The projectile fragmentation process

At energies higher than a few hundreds MeV/nucleon, the collision time becomes shorter than the velocity of the shock wave inside the nucleus. As a result, the overlapping region is just removed at the collision from the projectile nucleus, and the rest parts of the projectile nucleus fly away unaffected as schematically shown in Fig.1. So that, the velocity of the out going fragments are almost the same as that of the incident beam. This picture of the high energy heavy ion collisions is called the participant-spectator model, and this process is called the projectile fragmentation process. Because of the variety of the overlapping volumes, nuclei in a wide range of the nuclear chart are produced in the collision.

Because of kinematical focusing effect, the momentum distribution of the projectile fragments is very narrow compared with the initial momentum. It is well known that the width of the fragment momentum σ is well accounted for by the Fermi momenta of the nucleons inside a nucleus. The theoretical width based on the picture is given by Goldhaber [8] as;

$$\sigma = \sigma_0 \sqrt{\frac{A_F(A_P - A_F)}{A_P - 1}}, \qquad \sigma_0^2 = (3/5)\, p_F^2 , \tag{1}$$

where A_P and A_F denote the mass numbers of the projectile and fragment, respectively, and p_F is the Fermi momentum. The model implies isotropic momentum distribution. From the model, the longitudinal momentum spread $\Delta p/p$ is less than 1 % and the angular spread is less than 10 mr, in typical cases at E/A > 100 MeV/nucleon. Thus, the produced fragments can be easily transported down to the experimental area with a beam line, just like the primary beam.

b) Productivity

Isotope production with the projectile fragmentation process was clearly demonstrated in 1979 by Westfall et al. [9] in ^{48}Ca on ^{9}Be collisions. It was shown that a variety of nuclei could be produced using high energy heavy ion collisions. Even for nuclei very close to the neutron drip line, the production cross section was above 1 μb. The production cross section of a fragment in high energy heavy ion collisions is determined by the geometry of the collision and the stability of the fragment. The production of the fragment in the first abrasion stage is basically determined by the geometry of the overlapping region. After the abrasion, however, the fragment is in an excited state because of the sudden change in its shape, and decays by particle emission in the succeeding ablation stage. So, the ablation stage is largely dependent on the thresholds of particle emission, namely the instability of the fragment. The abrasion-ablation model [10] based on this picture along with the Glouber's scattering theory explains the experimental cross sections fairly well. Computer codes are also available for semi-empirical calculation based on this picture. The cross section is thus rather independent of the incident beam energy as long as the energy is sufficiently high, partly because the nucleon-nucleon scattering cross section is fairly constant at energies above 100 MeV/nucleon and partly because of a saturation effect.

Production cross sections of various sd-shell nuclei originated from the ^{40}Ca incident beam were calculated by a code (FRAGBNL [11]) as shown in Fig. 2. To know the production rate, one needs to consider the target thickness and the beam intensity. In a typical case, one can assume a reasonable target thickness of about 100 mg/cm^2 of ^{9}Be, which corresponds to an atomic density of about 7×10^{21}

atoms/cm^2 and a beam intensity of about 10^{12} particle/sec (pps), which is readily available from accelerators. So, the production rate will be about 7000 pps for a μb.

For the study of the hyperfine interactions, we need intense radioactive nuclear beams, because we lose yeilds by further selection of momentum and angle to get a polarization and/or by the solid angle of the radiation detectors. By choosing the best primary beam species, we may get sufficient production rate for the study. Fig. 2-(b) shows the production cross section of oxygen isotopes produced from several kinds of primary beams. As shown in the figure, the closer in mass to the desired nucleus the primary beam is, basically the more production one gets. Even the proton-drip-line nucleus ^{13}O can be produced at the rate of about 10^6 pps with an ^{16}O beam. The technique is, of course, powerful also in fp-shell and heavier nuclei.

3. SEPARATION TECHNIQUE

In order to use such radioactive secondary beams of projectile fragments for various kinds of studies, the beam must be purified by a proper separation technique. The Beam 44 fragment separator [12] was built at the LBL's Bevalac for this purpose.

All the fragment separators built for this purpose, including that at Beam 44, essentially consist of two parts for two kind of separation: one is rigidity analysis and the other is energy loss analysis. The rigidity analysis provides separation of the fragments based on the mass A over charge Z ratio (A/Z). The energy-loss analysis provides another separation based on the ratio ($A^{2.5}/Z^{1.5}$). These two kinds of

analyses are basically sufficient to separate out the single isotope, since the velocity v is very close to the primary beam as already mentioned in the previous section.

Since the velocity of a fragment is very close to the velocity v of the primary beam, the rigidity $B\rho$ of the fragment with atomic number Z and mass number A is given as;

$$B\rho = \frac{p}{Ze} = \left(\frac{m_u v}{e}\right)\left(\frac{A}{Z}\right), \qquad (2)$$

where p is the momentum of the fragment and m_u is the atomic mass unit, i.e. $m_u c^2$ = 931 MeV. So, the fragments are analyzed by the first dipole of the separator and focused on the different positions based on the mass over charge ratio (A/Z) of the fragments at the dispersive focus of the dipole.

The remaining fragments are then passed through an energy degrader. In order to treat precisely the energy loss in the degrader, the range R of the fragment is considered. The range R of the fragment is empirically given as [13];

$$R = k(A/Z^2)(E/A)^{\gamma} + CA\,, \qquad (2)$$

where constants k and C are only dependent on the material, and the power γ of the energy term is very close to 1.75 for the energy region from 50 through 100 MeV/nucleon. The range can be also expressed as a function of the rigidity $B\rho$ of the fragment as follows:

$$R = k'\left(\frac{Z^{1.5}}{A^{2.5}}\right)B\rho^{3.5} + CA, \qquad \text{where } k' = k\left(\frac{e^2}{2m_u}\right)^{1.75}. \qquad (3)$$

Therefore, the new rigidity $B\rho'$ after passing through the degrader with thickness d is ;

$$B\rho' = \left[B\rho^{3.5} - \left(\frac{d}{k'}\right)\left(\frac{A^{2.5}}{Z^{1.5}}\right)\right]^{\frac{1}{3.5}} \qquad (4)$$

The fragments were thus separated based on the ratio $(A^{2.5}/Z^{1.5})$ by the energy loss analysis followed by another rigidity analysis in the latter half of the separator. In order to get enough separation power, the second analyzing term in the equation has to be about a half of the first term. In order to keep the achromaticity of the final focus, the energy degrader have to be a wedge with a carefully designed thickness gradient.

Fig. 3 shows these two types of separations clearly. It was shown that the desired nucleus can be essentially separated out by these two kinds of analyses For the proton-rich fragments near the stability line, the energy loss analysis, i.e., the separation based on the ratio $(A^{2.5}/Z^{1.5})$ is almost the same as separation by neutron number N.

In Fig. 4, a schematic view of our fragment separator built at Beam 44 at the LBL's Bevalac is shown without focusing beam line elements. The first dipole provides the rigidity analysis. The energy degrader set at the intermediate focus and the succeeding rigidity analyzer, the second dipole magnet, provides the energy loss analysis. Fig. 5 shows typical data on the spatial distribution at the final focus of different fragments ^{37}K and ^{39}Ca, which are in the same A/Z group. These two different kinds of fragments were focused on the two different horizontal positions based on their $A^{2.5}/Z^{1.5}$ ratios. Either ^{37}K or ^{39}Ca were selected by defining the position at the final focus.

In order to tune the separator to the specific nucleus and transport them down to the experimental area correctly, we first have to identify each particle. This can be done by the measurement of the energy loss (ΔE) and the time of flight(TOF). Energy loss identifies Z^2, while TOF identifies velocity, namely the ratio A/Z, because the velocity of the fragments with the same rigidity is proportional to the ratio Z/A. So, the two dimensional map of TOF and ΔE give us particle identification. At the B44 fragment separator, energy loss was measured by a 400 μm thick SSD (Solid State Detector) and TOF was measured by a pair of plastic scintillation counters placed 8 m apart. A typical two dimensional map taken at the Beam 44 fragment separator is shown in Fig. 6. The fragments were successfully identified as marked. The two dimensional map deformed due to the energy loss at the intermediate focus. By a simple transformation of the two dimensional map, (Z) and (A/Z) were clearly identified as shown in the same figure.

The separation power of the present Beam 44 fragment separator is just enough for the $f_{7/2}$-shell nuclei (A<50). For the heavier nuclei, a separator with higher resolution is necessary. The fragment separator (FRS) at GSI has such a resolution, and in the future will be available for hyperfine studies. The GSI's FRS has successfully separated isotopes in the mass = 200 region [14].

4. ENERGY CONTROL

The produced radioactive nuclei have to be implanted in a sample for the various studies. Usually the kinetic energy of the fragments after the fragment separator is still too high to implant the fragments in the best depth. Therefore, we

need a suitable energy degrader in order to control the implantation depth. In the B44 separator, a thickness controllable plastic degrader was installed for this purpose. The energy degrader consists of two wedges placed face to face, so that the total thickness can be controlled by changing the relative position of these two wedges.

It is noted that the produced fragments are lost by the nuclear reaction in some level during the energy degradation and it becomes serious when the energy of the primary beam is higher than a few hundreds of MeV/nucleon. It is also noted that the energy spread in the beam of produced fragments is increased during the energy degradation process, because of the energy straggling and the energy defocusing effect in the energy degrader. A fragment with lower energy looses more energy than a fragment with higher energy, so that the energy difference between these two fragments is increased after the energy loss. The magnification of the energy spread due to this effect is determined by the ratio of the stopping power dE/dx at the exit of the energy degrader to that at the entrance. This effect becomes serious when one needs a low energy beam of probe nuclei.

The energy spread, however, can be refocused at some level using a so-called monochromatic wedge, with a specially designed gradient, as the energy degrader for energy-loss analysis. The wedge shaped energy degrader placed at the dispersive focus works as a energy compensator by introducing a larger energy loss to the higher energy particles. After the energy is reduced lower than 10 MeV/nucleon, another method becomes effective. Using a thin foil of high atomic number material like Au as the final energy degrader results in energy spread being refocused. At sufficiently low energies, energy loss is higher for the higher energy particle than the lower energy particles in general, so that we can expect the energy refocusing. Since the energy span of this kind of reverse feature in energy loss is wider for heavier materials, a Au foil is well suited for the purpose.

Such a energy refocus effect was successfully demonstrated in an experiment using ^{43}Ti. Energy spread in the ^{43}Ti beam which was originally ±3.6 MeV/nucleon at 92 MeV/nucleon was reduced to ±0.5 MeV/nucleon at 60 MeV/nucleon by the monochromatic wedge degrader, which, however, just correspond to ±3MeV/nucleon at the lowest energy. With the additional use of a thin Au foil of about 20 mg/cm^2 as a final degrader, the energy spread in the beam was further reduced, because of the negative curvature in the energy loss character for Au at energies below 5 MeV/nucleon. The resultant energy of the ^{43}Ti beam was reduced as low as 1.5 ± 1.0 MeV/nucleon. This kind of low energy beam is necessary for the Tilted Foil Technique to polarize the probe nuclei.

In this monochromatic condition, the achromatic condition is disturbed and the resolution of energy loss analysis is generally degraded. However, separation can be attained also by analyzing range of the particles directly. As shown in the range spectrum (Fig. 7), clear separation between several mirror nuclei were attained.

5 POLARIZATION TECHNIQUE

a) TFT polarization

For the present application of β-NMR, it is necessary to polarize the produced nuclei. For the creation of polarization, the Tilted Foil Technique (TFT) is supposed to be a good universal method [15]. The technique uses the polarization phenomenon in the orbital electrons around a nucleus passing through a foil surface through the asymmetric interaction between orbital electrons

and the electrons at the tilted foil surface. So, the energy of the nucleus should be low enough to put as many electrons around the nucleus as possible.

Since the first application of the TFT to the β-NMR technique, various data were accumulated. However, it was not clear whether the TFT works as the polarizer also at higher energies. Usually, the TFT polarization has been observed at energies below 300 KeV/nucleon. Such a low energy secondary beam was obtained by suitable energy degradation and proper energy compensation as mentioned in the previous section. Using the monochromatic wedge, the final energy was reduced to as low as 1.5 MeV/nucleon. We observed the tilted foil polarization created in ^{39}Ca [16] as shown in Fig. 8.

b) Reaction polarization

Another powerful method to polarize the fragments is to use the polarization phenomena in the heavy ion collisions. In the framework of the simple fragmentation model, polarization can be expected for the fragment ejected at a finite deflection angle. In order to introduce such deflection of the fragment, target nucleus with high atomic number such as Au was first used, expecting Coulomb deflection. At high energy, we measured the nuclear spin polarization of beta-emitting fragments at the finite deflection angles near the classical grazing angles. Polarization of about 5% was observed [17] for the beta-emitting fragments ^{37}K and ^{39}Ca produced in the ^{40}Ca on Au collision at 106 MeV/nucleon as shown in Fig. 9. The typical trend in fragment polarization with its momentum dependence was explained fairly well qualitatively by the simple model of the projectile fragmentation process.

In the case of the light target, fairly large polarization was also observed in ^{43}Ti fragments produced through ^{46}Ti on C collisions [18] as shown in Fig. 10. Unlike the case of the heavy target, the observed momentum dependence of polarization was a decreasing function. This trend can be explained by introducing the negative angle deflection of the fragments by the nuclear attractive potential. Thus, polarization can be created in the fragment selecting the deflection angles and momentum of the fragments regardless of the choice of target. However, the polarization may show different momentum dependence depending on the choice. As far as the production rate is concerned, the light target is preferable. So, we have to chose the optimum target for specific cases. For this kind of decision, information on the polarization mechanism is very important. Although the energy and the mass ranges are different, data from the intermediate energy region studied at RIKEN by Asahi et al. [19] are also helpful for the choice of the conditions.

6. RESULTS OBTAINED AND FUTURE

With the production and separation technique, a variety of nuclei can be produced and singled out for implantation into a catcher. As soon as we start counting beta rays, the decay life of the nuclide can be determined from the time spectra. As typically shown in Fig. 11, we obtained fairly clean time spectra. From time spectra, the half lives $T_{1/2}$ of ^{20,21}F, ^{37,39}Ca, and ^{43}Ti were determined to be 11.03± 0.05 sec, 4.21± 0.03 sec, 169.9± 9.4 msec, 864± 7 msec, and 503±8 msec, respectively [20].

We measured the magnetic moment of ^{43}Ti [21]. ^{43}Ti was produced through the projectile fragmentation process of the ^{46}Ti beam on the C target at 116

MeV/nucleon, and was polarized through the collision. NMR was detected for the ^{43}Ti implanted in a cooled Pt foil (90 K) under the external magnetic field of H_0= 5.878 kOe by means of asymmetric beta decay. As shown in Fig. 12, NMR effects were observed as a function of rf frequency. A resonance was found in the NMR spectrum at a frequency f= (1.27 ± 0.03) MHz. From the resonance frequency, the magnetic moment of ^{43}Ti was deduced to be $|\mu|$= (0.85 ± 0.02) μ_N. The value is significantly quenched from the single particle value -1.91 μ_N, which shows a strong effect resulting from meson exchange currents and configuration mixing. A shell model calculation with first order configuration mixing predicts - 0.754 μ_N [22], and the semi-empirical odd-nucleon model predicts - 0.784 μ_N [23], both of which reproduces the observed value fairly well.

The isoscalar and the isovector moments of the mirror pair were deduced to be $\mu^{(0)}$= 1.89(2) μ_N and $\mu^{(1)}$= -2.74(2) μ_N, from the moment of ^{43}Ti and ^{43}Sc. The shell model calculation [22] with first order configuration mixing predicts $\mu^{(1)}$= -2.71 μ_N, which agrees with the present value very well. However, this may not be an indication that the meson exchange effect is negligible, but that the second order configuration mixing effect almost cancels the meson exchange effect, as is in the case of the mass A=40±1 system.

Thus, the present technique has proven its effectiveness for the magnetic moment study of the $f_{7/2}$-shell-mirror nuclei. In the future, magnetic moments of mirror nuclei in $f_{7/2}$ shell will be measured by the present technique. There is special interest in the region near the closed shell A=56, which is the next to the well studied A=40 closed shell.

Recently, we found an anomalously large quadrupole moment in the proton-rich nucleus ^{8}B [24] produced through low energy nuclear reactions. The large Q moment (Q_{exp}=68.3±2.1 mb) is explained only by the existence of the proton halo

covering the ^{7}Be core. This was the first positive evidence of a proton halo, because high energy reaction cross sections failed to detect such a structure, unlike the famous neutron halo. Thus, Q-moments are very important in studying the proton halo structure of the proton-rich nuclei

The Q-moment measurement was not so easy previously because of the small NMR effects due to the quadrupole splitting of the NMR spectra. Now, a new development has been made in the β-NMR technique. Briefly, in the new technique [6], all the transitions of the split lines by the eqQ interaction was induced repetitively. By this procedure, the polarization is totally destroyed. Compared with the conventional method, where the single rf was applied to one of the split lines, the efficiency was improved dramatically. Compared with the conventional β-NMR, the new technique is more efficient by the factor of $(8/9)I^3(I+1)^2(2I+1)^2$ for the spin I. A similar technique was used at CERN ISOLDE independently, for the study of the Q moment of the very neutron-rich nucleus of ^{11}Li [7]. Because of the new NQR technique, the application of the present production technique to the Q moment measurement is realistic. Since the interesting proton-rich nuclei lies on the proton-drip line, the present production technique through heavy ion collisions is the only way to reach there. So, we urge application of this technique for further studies.

Since the present technique can be applicable to any kind of β-NMR studies, other areas of hyperfine interaction can also be studied using the variety of β-NMR probes now available. Examples include studies of the hyperfine field in ferromagnetic samples, determination of implantation sites for very dilute impurities, studies of damages and defects in semi-conductors, studies of electronic structures in ionic crystals through quadrupole interactions, etc.

It is well established that the Fermi coupling constant for nuclear beta decay is smaller than the pure leptonic decay of the muon, by the factor of $\cos\theta_c$ [25], where the θ_c is the strength dividing angle between nuclear beta decay and the hyperon decay. Since the discovery of an anomaly [26] in the coupling constant determined from the spin non-zero ^{35}Ar decay as shown in Fig. 13, however, it has become an open problem whether the restoration from the symmetry breaking occurs under the extremely strong (10^{15} T) electromagnetic force [27] expected in such a spin non-zero nucleus. For this experiment, both the decay rate and the asymmetry parameter have to be measured. For this investigation, the most appropriate candidate is ^{23}Mg (I^{π}=3/2^{+}, $T_{1/2}$=11.32 sec), since the beta-decay branch to the first excited state is relatively large, which is necessary for the precise determination of the polarization. Since the present technique is most promising to provide the polarized ^{23}Mg efficiently, this study is urged.

Along with the ISOL techniques, NO or NMR-ON, Laser pumping in solids, transient field, mechanism of TFT, application to ion trap, Mössbauer spectroscopy, PAC, PAD, etc. have to join in to expand the field of hyperfine studies using the variety of probes available through the relatively new, but promising production technique.

7. LIMITATIONS OF THE PRESENT TECHNIQUE AND POSSIBLE SOLUTION

By now, the mass range of the nuclei which can be efficiently separated is up to 60 or so, using the B44 fragment separator. For heavier nuclei other facilities like RIPS, RIKEN can be used. Although they have not tried yet, the RIPS have such a

capability. GSI's FRS has already demonstrated the separation of the isotopes in mass A= 200 region, although its energy is too high for the present purpose.

Another limitation is the purity of the separated nuclei. At GSI's energy, the separator performed well as mentioned above. Below 100 MeV/nucleon, however, imperfect momentum focusing is serious problem in obtaining a high purity beam. In other words, the spread in the velocity of the fragment is not sufficiently small to have good separation. This problem is exacerbated by the fact that at least one of the neighboring unwanted isotopes has a more than 10 times larger production cross section than the desired probe nucleus. The problem can be avoided by introducing a velocity filter in the separator, as is in the LISE3 at GANIL. For such an experiment, which needs high purity beam, this is the only way presently, until deceleration in the GSI cooler ring becomes realistic.

Although, the present production technique is universal in its ability to produce virtually any unstable nuclei, the production rate becomes very small for extremely unstable nuclei. It is thus necessary to plan the experiment with a realistic estimation of the production rate.

Because of the conflicting situation between high production energies and the relatively low implantation energies, presently attainable lowest implantation energy is 1.5 ±1.0 MeV/nucleon (± denotes the width of the distribution), which was demonstrated at the B44 fragment separator. However, the energy spread is larger than that required for some applications like TFT polarization. RIKEN's RIPS may have such capability, though it is still untested.

8. Summary

The projectile fragmentation process can be a good tool to provide a variety of probe nuclei for studies on hyperfine interactions. Its advantage comes mainly from the universally high productivity for such nuclei and the fast analysis capability of about a micro second. Its has, however, limitations on the mass range, on the productivity of extremely unstable nuclei, on the purity of the probe nuclei, and the controllability of the final kinetic energy. Although it is not a easy job, these problems can be improved with the improvement of the accelerator's energy spread and the improvement of the fragment separator. In spite of these limitations, the effectiveness is evident and is already widely used for nuclear physics as well as magnetic moment studies.

Since the β-NMR method was recently improved, the efficient measurement of the Q moment became possible. The combination of the nuclear physics technique and the hyperfine interaction technique can be also applied to study the symmetry in basic interactions, especially the weak interaction. The other powerful technique, i.e., the post acceleration after the ISOL type facility is now under planning and construction. This kind of facility has higher mass resolution and purity, although the analysis speed is limited in some cases. In this sense, this technique will be a counter part to the present technique. It is possible, promising, and we urge the utilization of these techniques/facilities for the expansion of the study of hyperfine interactions.

Acknowledgments

The present work was supported by the Grant in Aid for Scientific Research, the Monbusho International Science Research Program, and the special project for Isotope Beam Science from the Ministry of Education, Culture and Science, Japan. Support was also given by the U.S.A.-Japan Collaborative Research, funded by both the Japan Scientific Foundation, and the National Science Foundation, U.S.A. It was also supported in part by the US Department of Energy, under contract No. DE-AC03-76SF0098, and by the Kurata Research Grant from the Kurata Foundation.

References

[1] H.L. Ravn, Phys. Rep. 54 (1979) 201.

[2] W.F. Rogers, D.L. Clark, S.B. Dutta, and A.G. Martin, Phys. Lett. B177 (1986) 293; Nucl. Instr. Meth. in Phys. Res. A253 (1987) 256.

[3] Y.P. Viyogi, T.J.M. Symons, P.Doll, D.E. Greiner, H.H. Heckman, D.L. Hendrie, P.J. Lindstrom, J. Mahoney, D.K. Scott, K. Van Bibber, G.D. Westfall, H. Wieman, H.J. Crawford, C. McParland, and C.K. Gelbke, Phys. Rev. Lett. 42 (1979) 33

[4] D. Guerreau, Journal de Physique, Suppl. 8, C4 (1986) 207.

[5] I. Tanihata, Nucl. Phys. A 522 (1991) 275c.

[6] S. Fukuda, T. Ohtsubo, N. Nakayama, M. Tanigaki, A. Kitagawa, Y. Someda, S. Takeda, M. Fukuda, K. Matsuta, Y. Nojiri, and T. Minamisono, Annual Report OULNS-1990 (1991) 76.

[7] E. Arnord, J. Bonn, A. Klein, R. Neugart, M. Neuroth, E.W. Otten, P. Lievens, H. Reich, W. Widdra, and ISOLDE Collaboration, Phys. Lett. B 281 (1992) 16.

[8] A.S. Goldhaber, Phys. Lett. 53B (1974) 306.

[9] G.D. Westfall, T.J.M. Symons, D.E. Greiner, H.H. Heckman, P.J. Lindstrom, J. Mahoney, A.C. Shotter, D.K. Scott, H.J. Crawford, C. McParland, T.C. Awes, C.K. Gelbke, and J.M. Kidd, Phys. Rev. Lett. 43 (1979) 1859.

[10] J. Hüfner, K. Schäfer, and B. Schürmann, Phys. Rev. C 12 (1975) 1888.

[11] Code FRAGBNL is based on;
R. Silberberg and C.H. Tsao, the Astrophysical Journal Suppl. 25 (1973) 315.

[12] Y. Nojiri, K. Matsuta, T. Minamisono, K. Sugimoto, K. Takeyama, H. Hamagaki, S. Nagamiya, K. Omata, Y. Shida, I. Tanihata, T. Kobayashi, S. Matsuki, S. Shimoura, J.R. Alonso, G. Krebs, and T.J.M. Symons, Hyperfine Interactions 35 (1987) 1019,
K. Matsuta, J.R. Alonso, G.F. Krebs, T.J.M. Symons, M. Izumi, Y. Nojiri, T. Minamisono, A. Kitagawa, A. Ozawa, S. Momota, Y. Matsuo, T. Ohtsubo, K. Sugimoto, I. Tanihata, K. Omata, Y. Shida, S. Shimoura, and T. Kobayashi, Proc. 1st Int. Conf. on Radioactive Nuclear Beams, Berkeley, USA 1989, Edited by W.D. Myers, J.M. Nitschke and E.B. Norman (World Scientific, Singapore, 1990) p. 575.

[13] J.P. Dufour, R. Del Moral, H. Emmermann, F. Hubert, D. Jean, C. Poinot, M.S. Pravikoff, A. Fleury, H. Delagange, and K.-H. Schmidt, Nucl. Instr. Meth. in Phys. Res. A248 (1986) 267.

[14] K. Sümmerer, H. Geissel, K.-H. Behr, T. Brohm et al., Proc. 2nd Int. Conf. on Radioactive Nuclear Beams , Aug. 19-21, 1991, Louvain-la-Neuve, Belgium, Ed. Th Delbar, (IOP Publishing Co., London, 1992) p. 78.

[15] Y. Nojiri and B.I. Deutch, Phys. Rev. Lett. 51 (1983) 180,
Y. Nojiri, K. Takeyama, K. Matsuta, K. Asahi, and T. Minamisono, J. Phys. Soc. Japan 55 suppl. (1986) 391.

[16] Y. Nojiri, K. Matsuta, T. Minamisono, K. Sugimoto, K. Takeyama, K. Omata, Y. Shida, I. Tanihata, T. Kobayashi, S. Nagamiya, K. Ekuni, S. Shimoura, J.R. Alonso, G.F. Krebs, and T.J.M. Symons, Nucl. Intr. Meth. in Phys. Res. B33 (1988) 193.

[17] K. Matsuta, A. Ozawa, Y. Nojiri, T. Minamisono, M. Fukuda, A. Kitagawa, S. Momota, T. Ohtsubo, Y. Matsuo, H. Takechi, S. Fukuda, I. Minami, K. Sugimoto, I. Tanihata, K. Omata, J.R. Alonso, G.F. Krebs, and T.J.M. Symons, Phys. Lett. B 281 (1992)214.

[18] K. Matsuta, A. Ozawa, Y. Nojiri, T. Minamisono, M. Fukuda, S. Momota, T. Ohtsubo, S. Fukuda, K. Sugimoto, I. Tanihata, K. Yoshida, K. Omata, J.R. Alonso, G.F. Krebs, T.J.M. Symons, Proc. Int. Conf. on NFFS-12 and AMCO-9, Germany, also see Contribution to this Conference titled "Fragment Polarization of ^{43}Ti in the ^{46}Ti + C Collision".

[19] K. Asahi, M. Ishihara, N. Inabe, T. Ichihara, T. Kubo, M. Adachi, H. Takanashi, M. Kouguchi, M. Fukuda, D. Mikolas, D.J. Morrissey, D. Beaumel, T. Shimoda, H. Miyatake, and N. Takahashi, Phys. Lett. B 251 (1990) 488, M. Ishihara, Nucl. Phys. A538 (1992) 309c.

[20] K. Matsuta, K. Takeyama, M. Izumi, Y. Nojiri, T. Minamisono, A. Kitagawa, A. Ozawa, S. Momota, Y. Matsuo, T. Ohtsubo, K. Sugimoto, I. Tanihata, K. Omata, Y. Shida, S. Shimoura, K. Ekuni, T. Kobayashi, J.R. Alonso, G.F. Krebs, and T.J.M. Symons, Proc. 1st Int. Conf. on Radioactive Nuclear Beams, Berkeley, USA 1989, Edited by W.D. Myers, J.M. Nitschke and E.B. Norman (World Scientific, Singapore, 1990) p. 366.

[21] K. Matsuta, A. Ozawa, Y. Nojiri, T. Minamisono, M. Fukuda, S. Momota, T. Ohtsubo, S. Fukuda, K. Sugimoto, I. Tanihata, K. Yoshida, K. Omata, J.R. Alonso, G.F. Krebs, and T.J.M. Symons, Contribution to this conference titled "Beta-NMR Detection of Beta-Emitting Fragment ^{43}Ti".

[22] H. Miyatake, K. Ogawa, T. Shinozuka, and M. Fujioka, Nucl. Phys. A470 (1987) 328.

[23] S.M. Perez, Phys. Rev. C 36 (1987) 1202.

[24] T. Minamisono, T. Ohtsubo, I. Minami, S. Fukuda, A. Kitagawa, M. Fukuda, K. Matsuta, Y. Nojiri, S. Takeda, H. Sagawa, and H. Kitagawa, Phys. Rev. Lett. C69 (1992) 2058.

[25] N. Cabbibo, Phys. Rev. Lett. 10 (1963) 531.

[26] F.P. Calaprice, E.D. Commins, and D.A. Dobson, Phys. Rev. 137 (1965) 1453.

[27] A. Salam, Nature 252 (1974) 596.

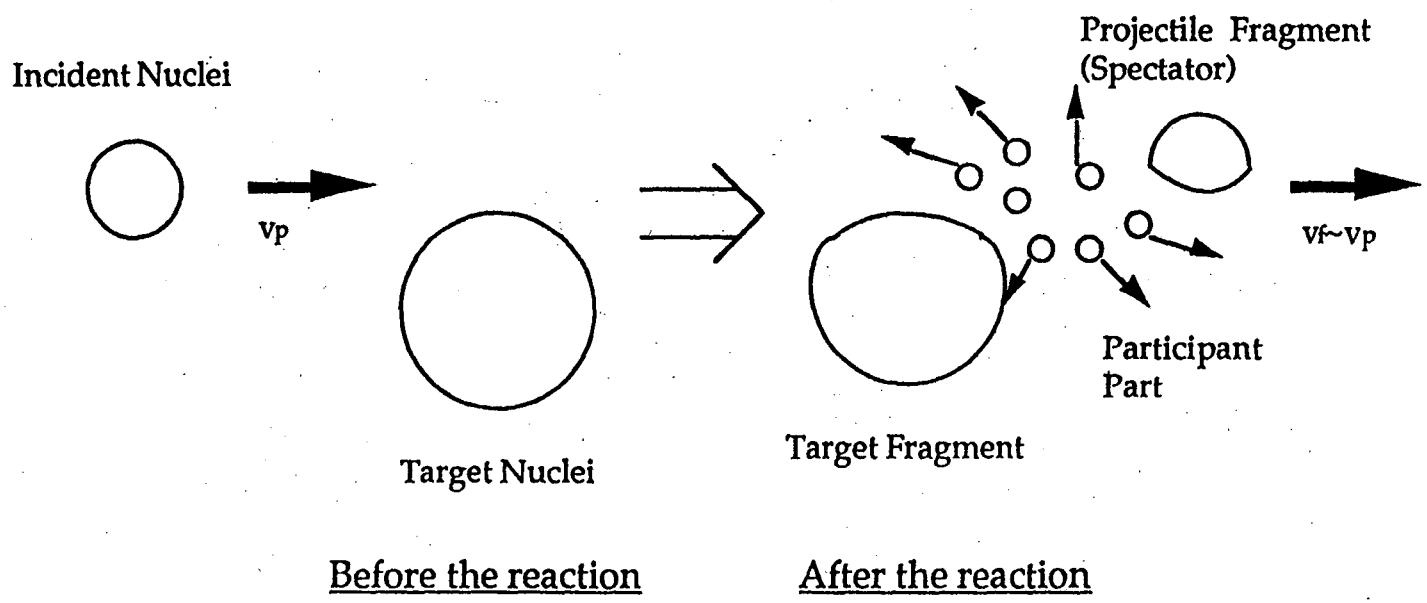

Fig. 1. Schematic explanation of the projectile fragmentation process.

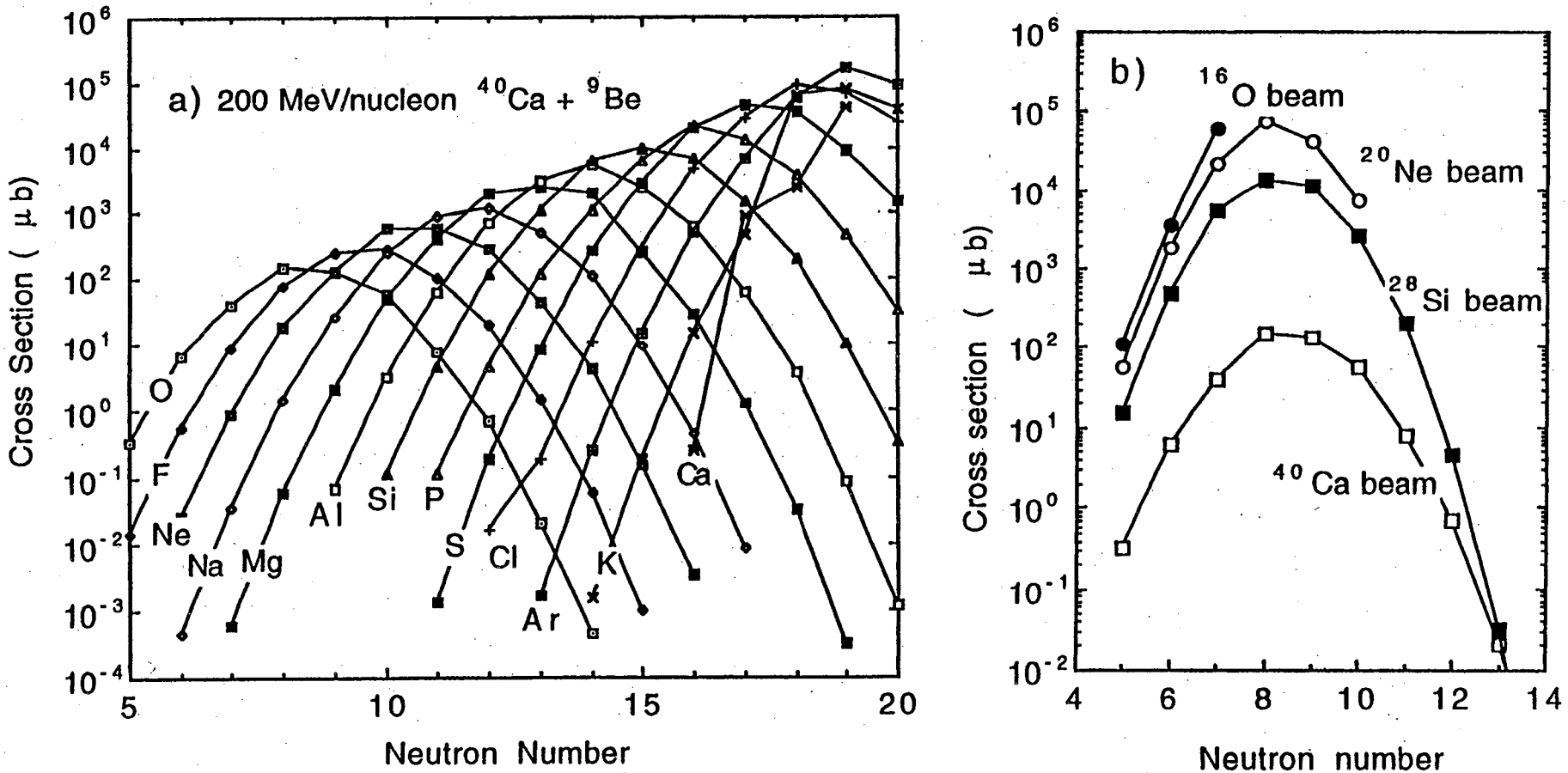

Fig. 2. Estimated production cross sections for sd-shell nuclei.

a) The cross sections were calculated for the 200 MeV/nucleon ^{40}Ca on ^{9}Be collisions by the code FRAGBNL.

b) Cross sections of O isotopes from different primary beams.

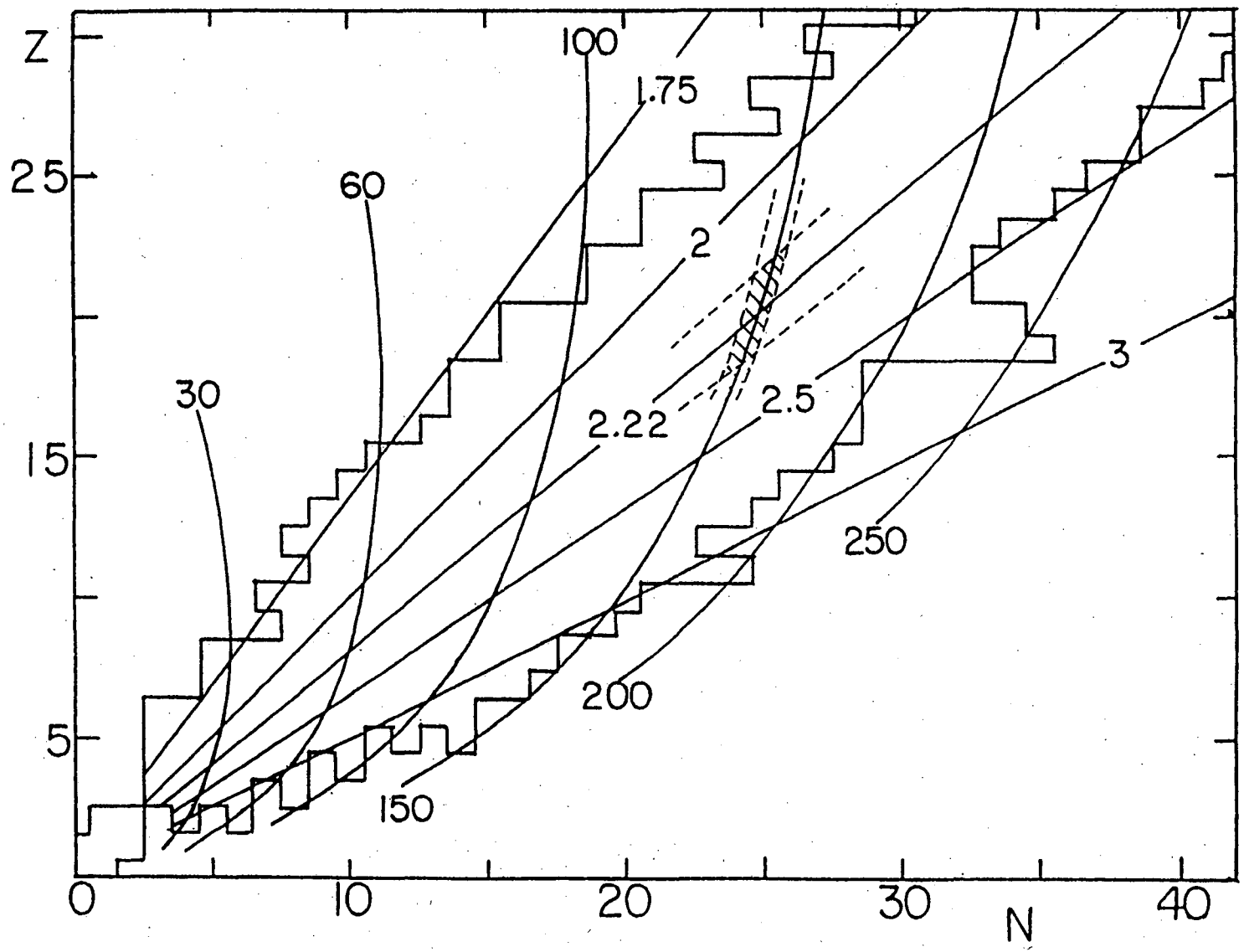

Fig. 3. Demonstration of the combined analysis.

The figure was taken from the reference [13].

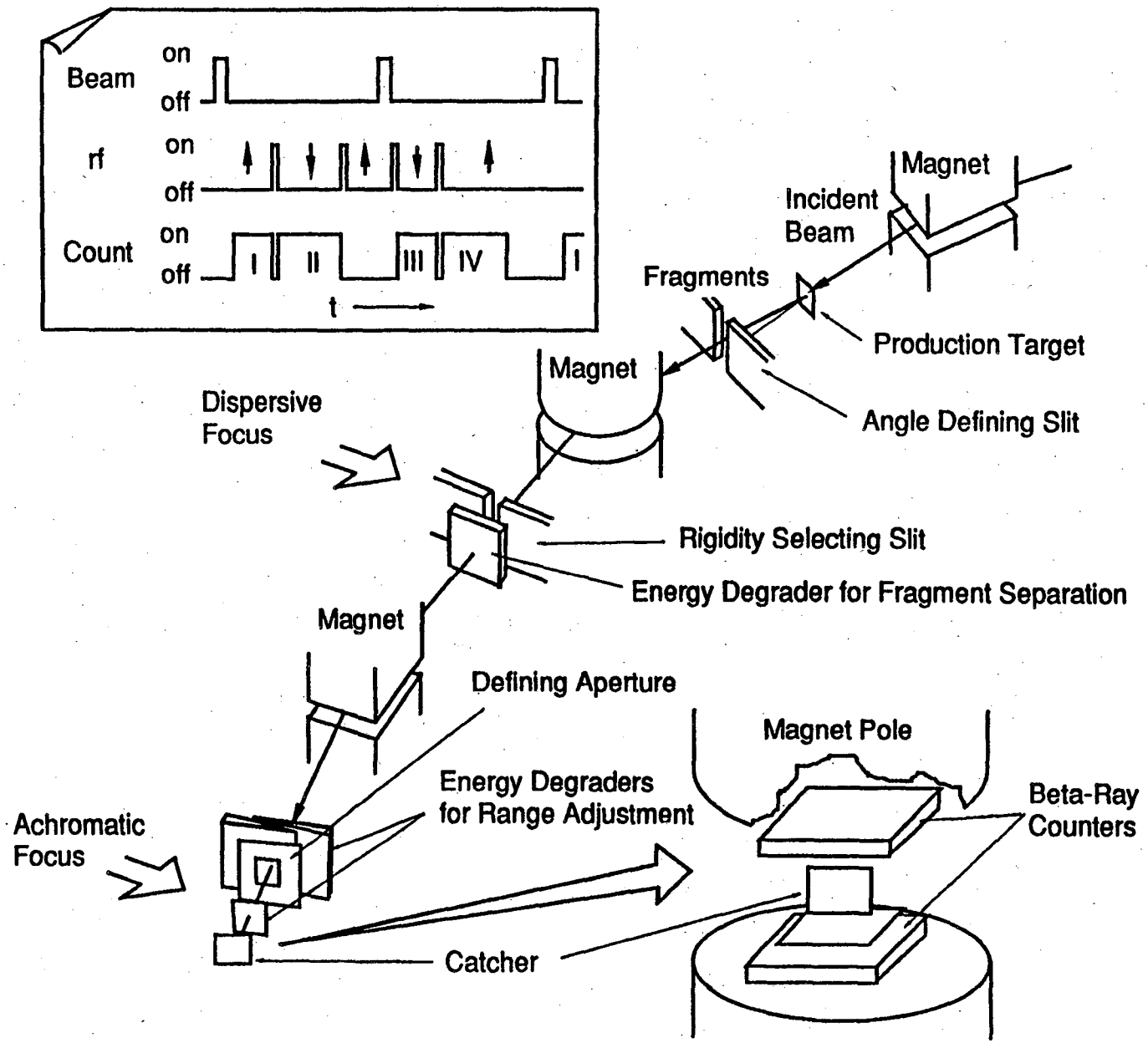

Fig. 4. B44 fragment separator.

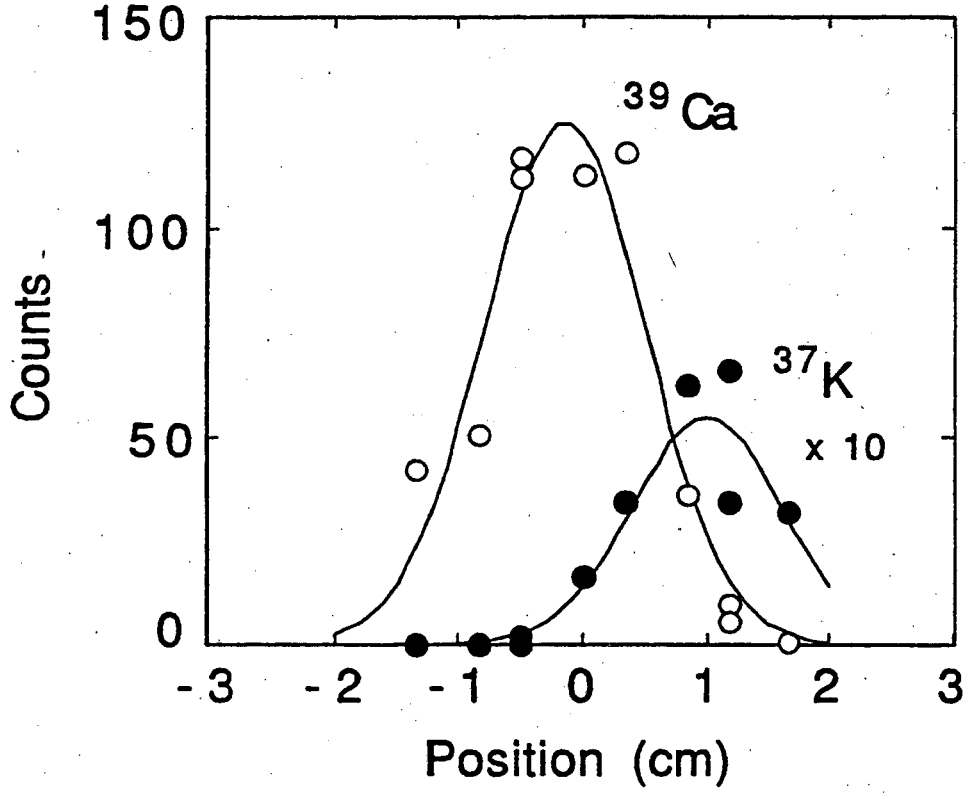

Fig. 5. Separation between ^{39}Ca and ^{37}K at the final focus of the B44 separator.

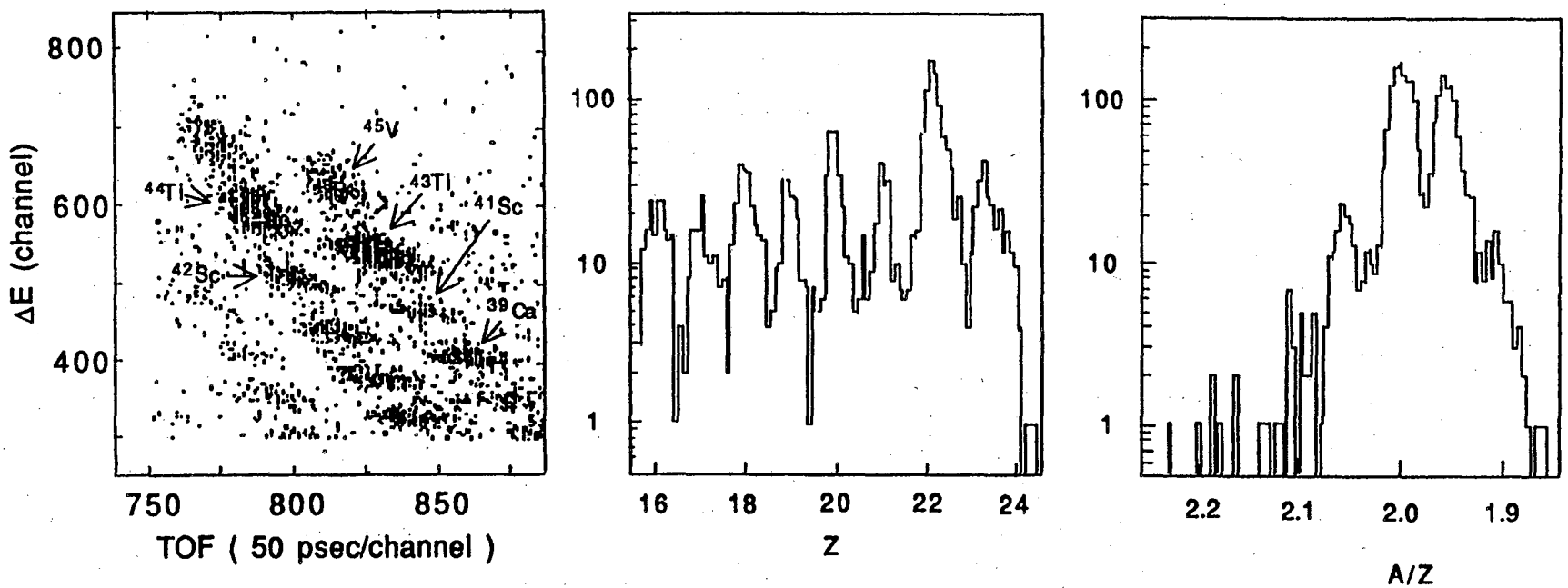

Fig. 6. Particle identification.

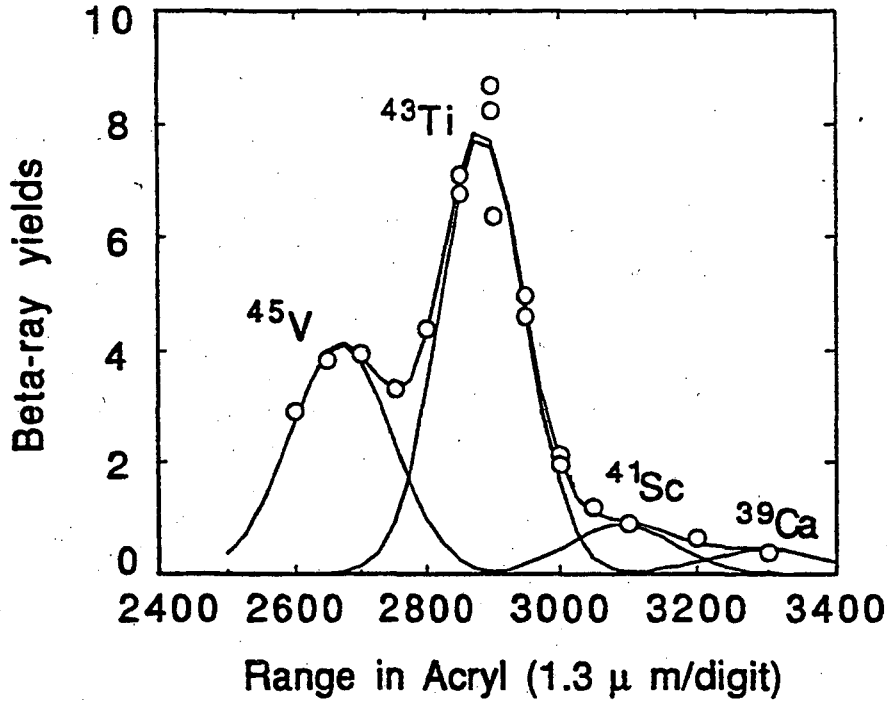

Fig. 7 Range distributions for several mirror nuclei.

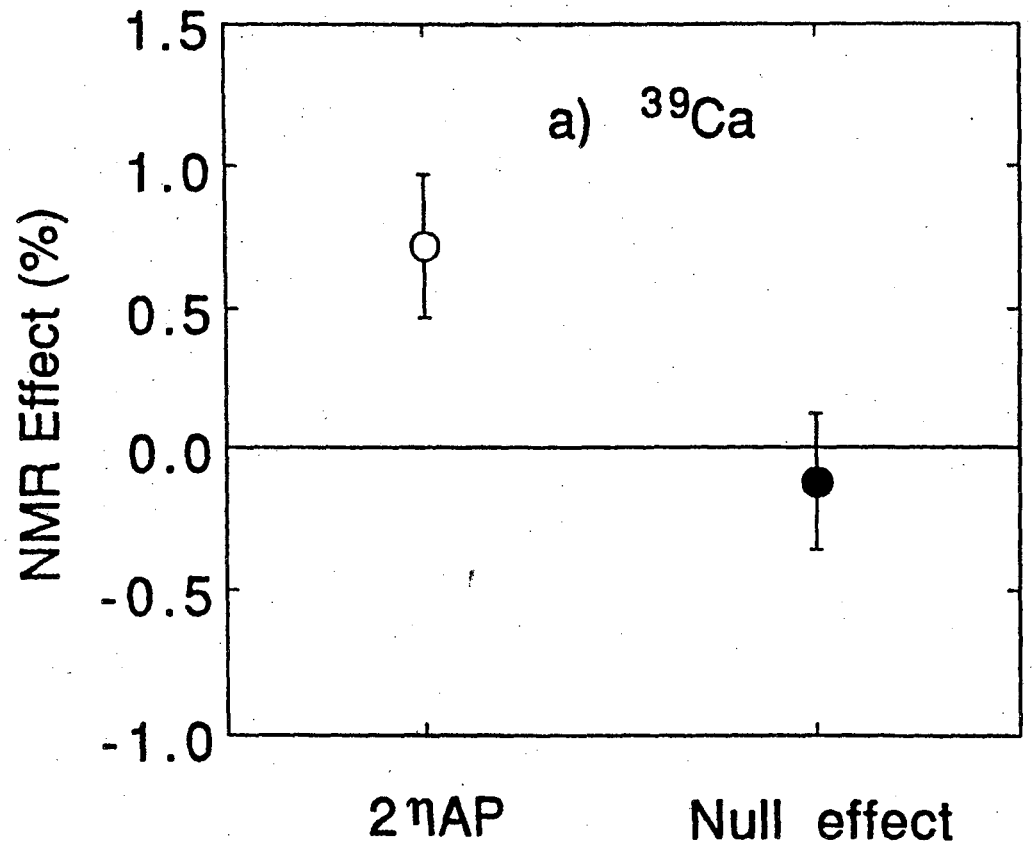

Fig. 8. TFT polarization of ^{39}Ca fragment.

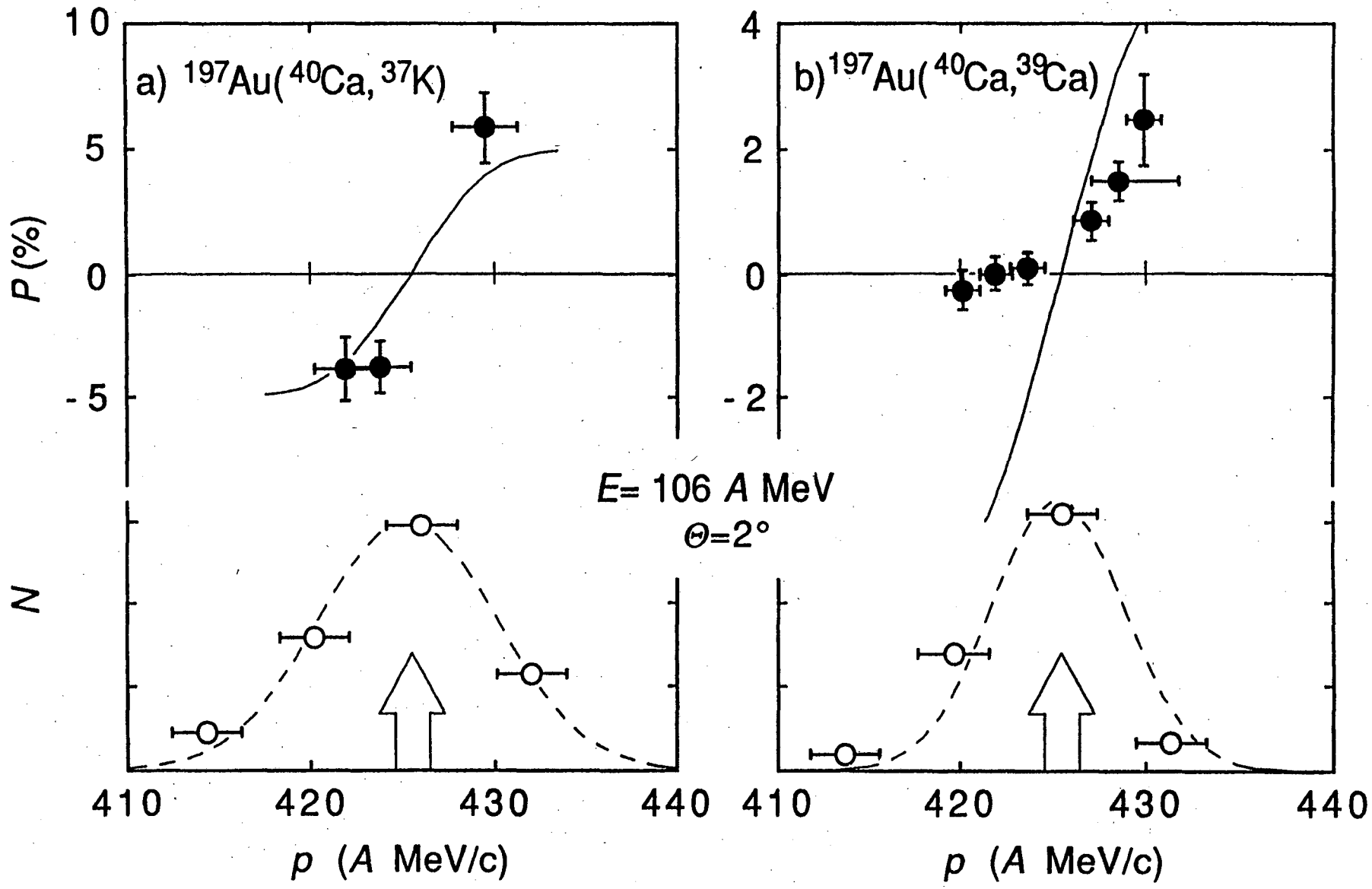

Fig. 9. Fragment polarization of ^{37}K and ^{39}Ca.

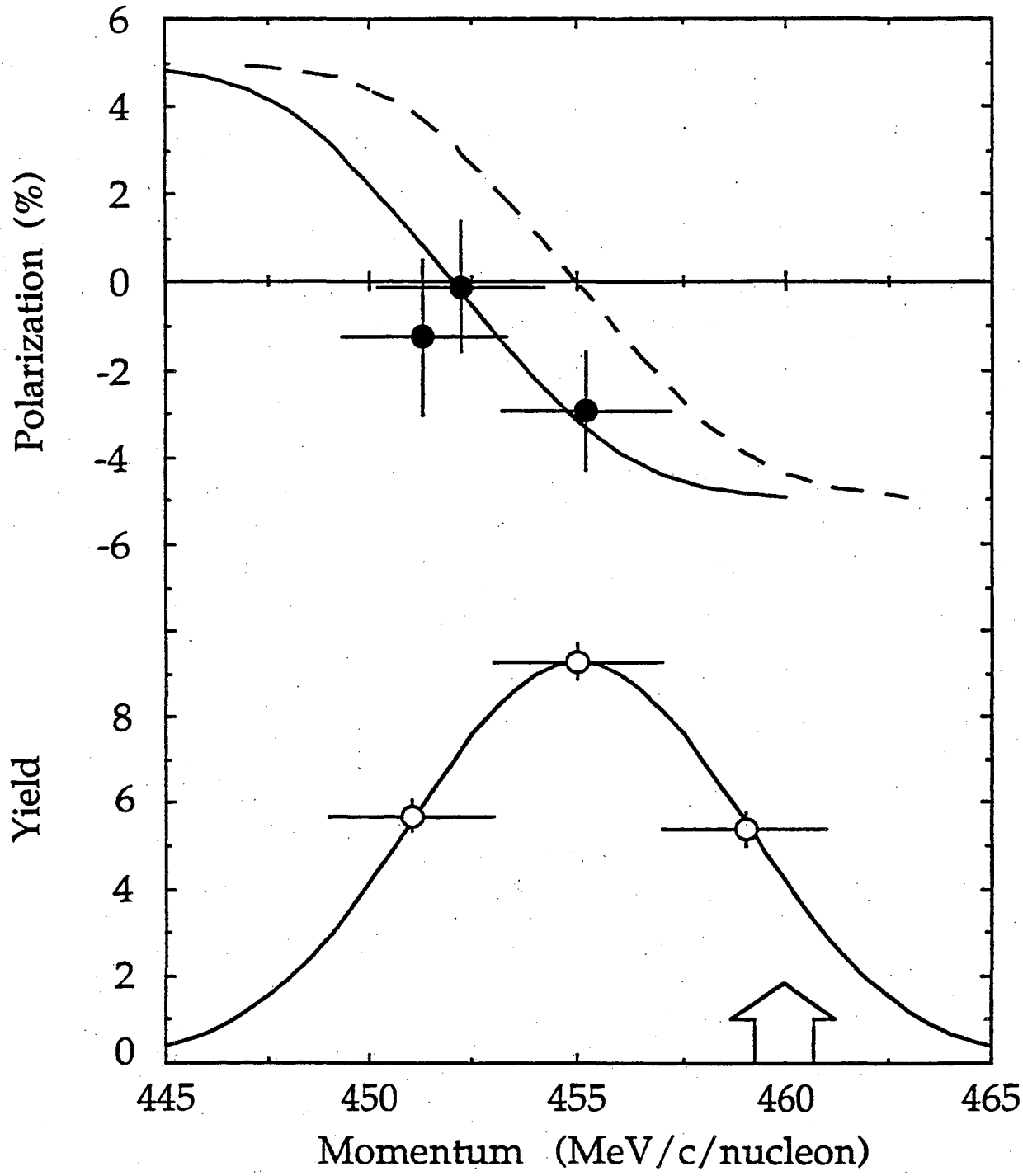

Fig. 10. Fragment polarization of ^{43}Ti.

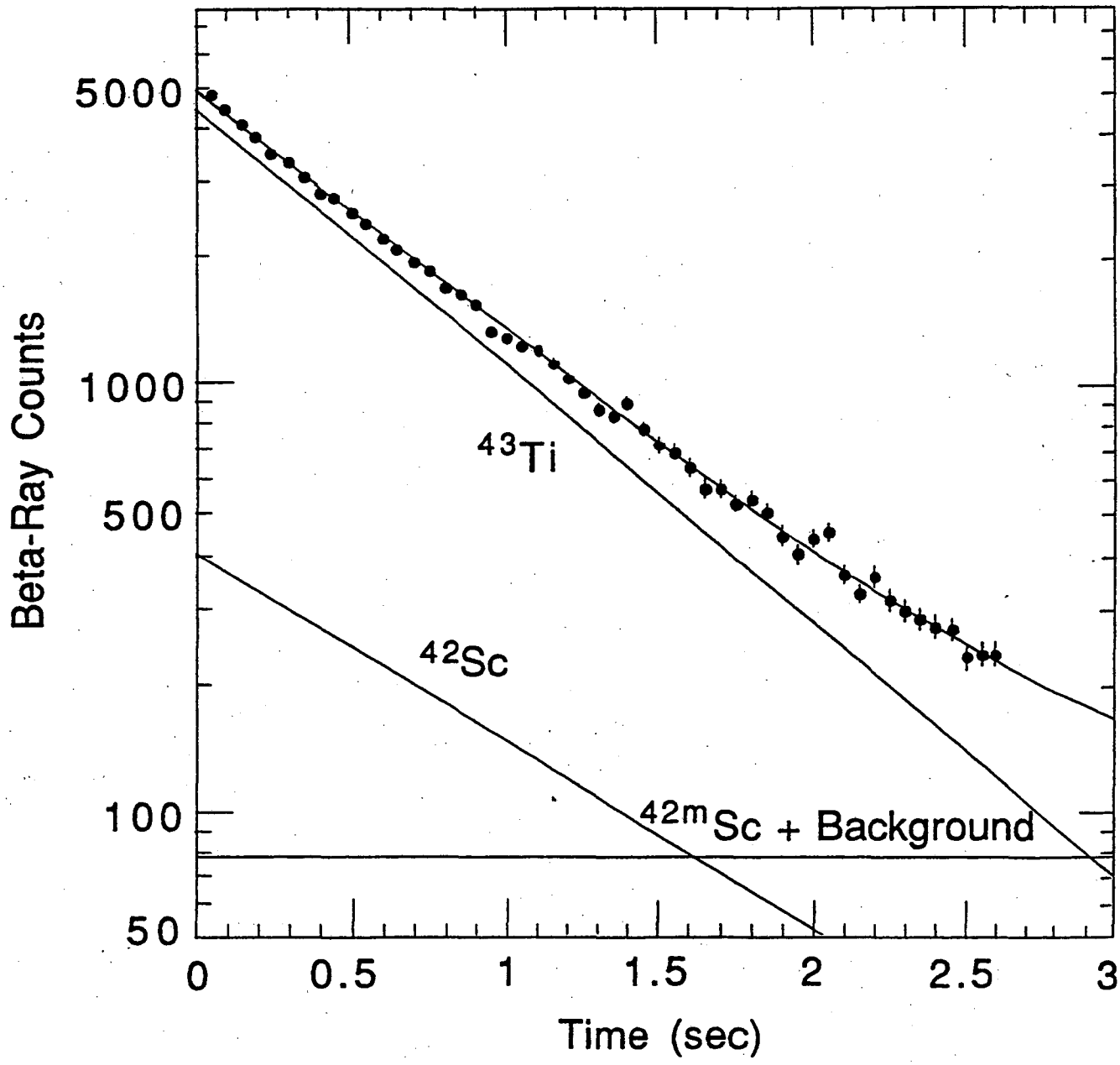

Fig. 11. Typical time spectrum for ^{43}Ti.

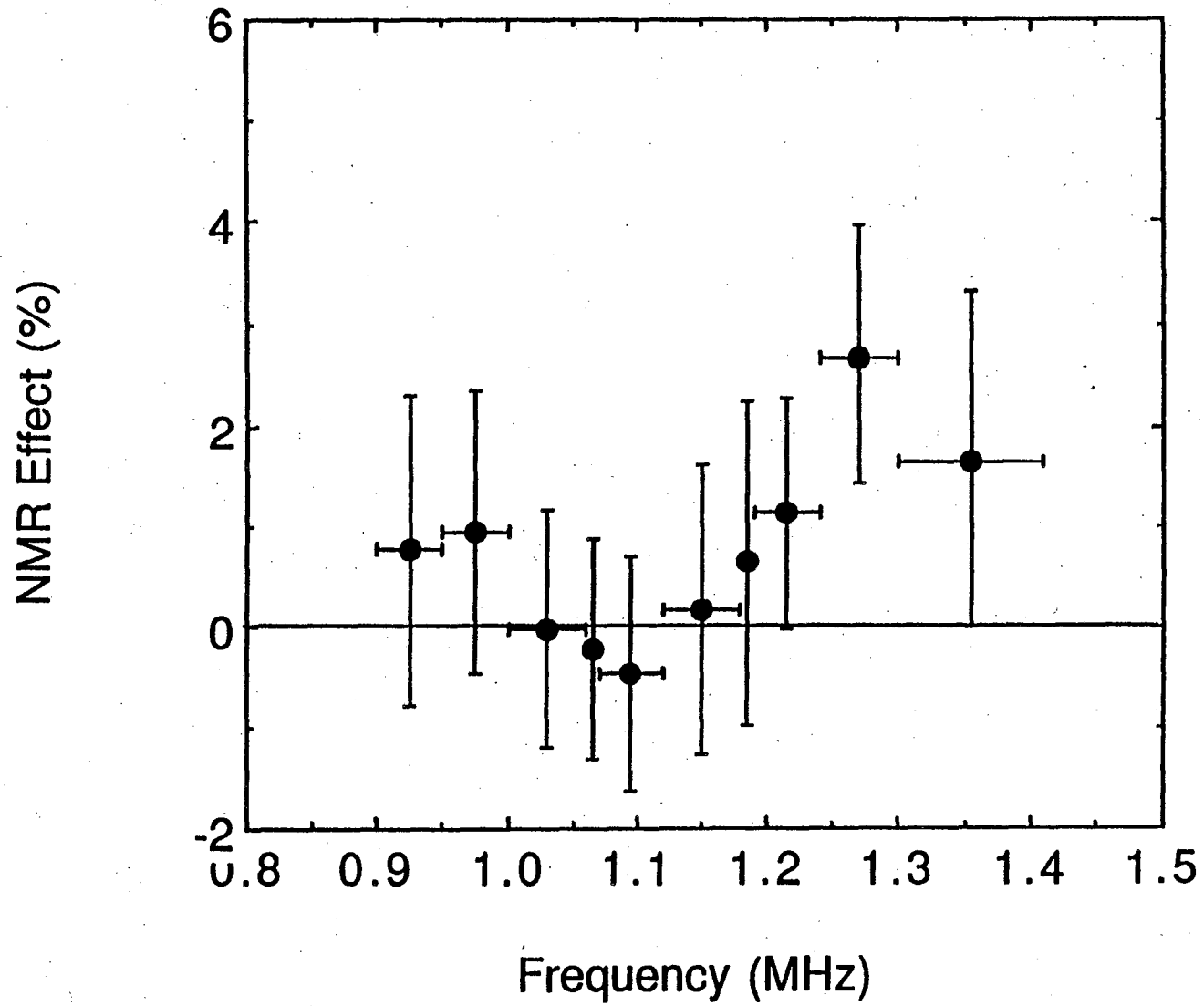

Fig. 12. NMR spectrum of ^{43}Ti.

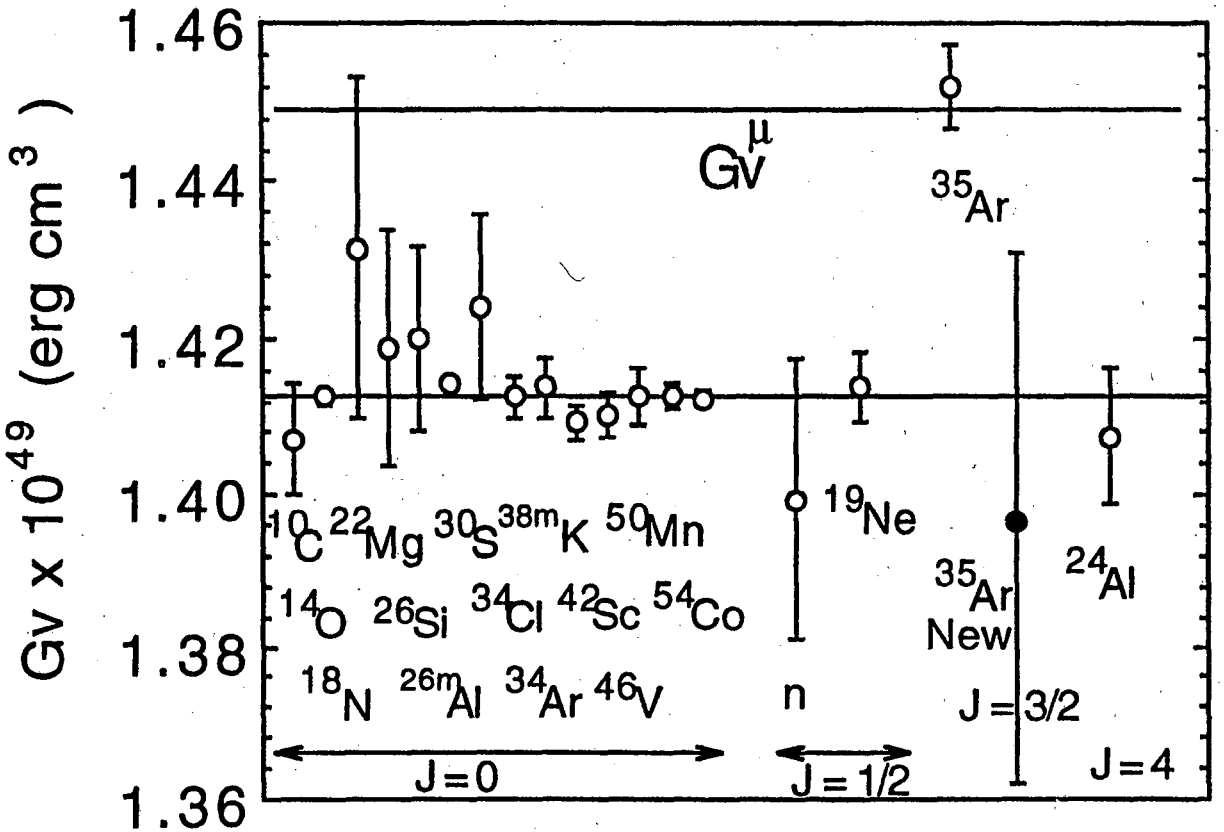

Fig. 13. Fermi coupling constant C_V determined from various nuclear beta decays.

LAWRENCE BERKELEY LABORATORY
UNIVERSITY OF CALIFORNIA
TECHNICAL INFORMATION DEPARTMENT
BERKELEY, CALIFORNIA 94720